Subwavelength metal structures with tunable transmission characteristics by light

Zehua Yang (杨泽华), Jing Han (韩 晶), Wenzhi Wu (吴文智), Degui Kong (孔德贵), and Yachen Gao (高亚臣)*

College of Electronic Engineering, Heilongjiang University, Harbin 150080, China
**Corresponding author: gaoyachen@hlju.edu.cn*

Received August 2, 2019; accepted August 30, 2019; posted online December 4, 2019

Extraordinary optical transmission (EOT) in subwavelength metal structures has been studied widely. Herein, we propose a strategy for tuning the EOT of the bullseye structure. Specifically, the bullseye structure was immersed in a nonlinear medium, and a controlling light was employed to change the refractive index of the medium. At different intensities and distributions of controlling light, the transmission property of signal light in the bullseye structure was simulated. The results show that a variable transmission spectrum in the bullseye structure can be realized. Moreover, the position of the central transmission peak shifts linearly with the increasing intensity of controlling light.

OCIS codes: 230.3990, 130.6010.
doi: 10.3788/COL201917.122302.

In 1998, Ebbesen *et al.* reported extraordinary optical transmission (EOT) in the subwavelength metal structures with periodic hole arrays[1,2] for the first time. Since then, extensive research on the transmission in subwavelength structures has been carried out[3–15]. People have studied EOT phenomena in different aperture arrays such as circles, rectangles, ellipses, and triangles. In addition, the EOT in some special subwavelength structures such as groove arrays and bullseye structures has also caused widespread concern due to their easy processing and high transmission. Based on the theoretical and experimental studies, EOT has been widely employed in selective lenses, optical switches, enhanced nonlinearity, and other novel sensors[15–23].

Although the physical mechanism of EOT is not completely clear, it has been recognized that the shape and size of the hole, the period of the groove, the material of the film, and the refractive index of the environment have a significant effect on the transmission characteristics. Once a structure and the parameters of the structure are proposed, the transmission characteristics of the structure are fixed. It is impossible to achieve dynamic regulation of their transmission continuously. People have to etch a variety of samples with different parameters for different requirements.

In this Letter, we propose a strategy to adjust the transmission of a subwavelength metal structure by employing external light. Because the bullseye structure[24] is a typical subwavelength structure and it has been widely applied in many fields[16,17] such as selective lens and novel sensor, we use it as an example to verify the validity of this solution.

As shown in Fig. 1, we design a bullseye structure on a silicon dioxide substrate. The whole structure covers an area with a 300 nm thickness. A hole with a radius of 150 nm is located in the center of the film surrounded by a groove with a depth of 60 nm and a period of 600 nm.

As shown in Fig. 2, we immerse the bullseye in carbon disulfide (CS_2), which is known as a typical nonlinear medium with a relatively larger nonlinear refractive index. In the external light field, the total refractive index n of CS_2 is expressed as[25]

$$n = n_0 + \frac{n_2}{2}\left|E^2\right| = n_0 + \gamma I, \tag{1}$$

where n_0 is the linear refractive index that is 1.6276, n_2 is nonlinear refractive parameter, E is the peak electric field (cgs), and I denotes the irradiance (MKS) of the laser beam within the sample. γ and n_2 are related through the conversion formula $n_2\,(\text{esu}) = (cn_0/40\pi)\gamma\,(m^2/\text{W})$, where $c\,(\text{m/s})$ is the speed of light in vacuum, at a wavelength of 800 nm, and γ is $2.1 \times 10^{-7}\,\mu\text{m}^2/\text{W}$[26]. From Eq. (1), we can see that the refractive index of CS_2 will vary with the intensity of the controlling light. Here we use a plane light with a wavelength of 800 nm and a power of 10^5–10^6 W as the controlling light to adjust the refractive index of the CS_2.

Using the finite-difference time-domain (FDTD) method, we simulate the transmission of the structure for a signal light (from 600 nm to 1300 nm) at five different controlling lights with power densities of $0\,\text{W}/\mu\text{m}^2$, $2.38 \times 10^5\,\text{W}/\mu\text{m}^2$, $4.76 \times 10^5\,\text{W}/\mu\text{m}^2$, $7.14 \times 10^5\,\text{W}/\mu\text{m}^2$, and $9.52 \times 10^5\,\text{W}/\mu\text{m}^2$, which make the nonlinear refractive index of CS_2 increase up to 0 RIU, 0.05 RIU, 0.1 RIU, 0.15 RIU, and 0.2 RIU, respectively. The corresponding transmission characteristics of the bullseye structure obtained are shown in Fig. 3.

In Fig. 3, we find that when there is no controlling light the transmission spectra have two peaks; the first one is at 930 nm, and the second one is at 1097 nm. Compared with the 660 nm measured by Lezec *et al.* in air instead of CS_2[27], obviously, the transmission peaks redshift because the structure was immersed in CS_2. When the controlling light

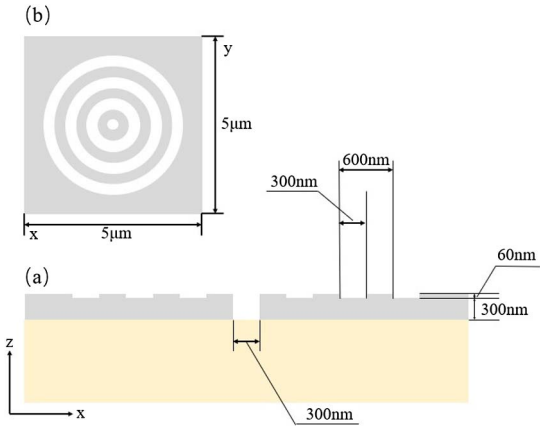

Fig. 1. Cross section of the bullseye structure (a) x-z cross section (elevation view) and (b) x-y cross section (top view).

with the power density of $2.38 \times 10^5\,\mathrm{W/\mu m^2}$ is introduced, the first peak redshifts to 949 nm, and the second to 1162 nm. As the power density of the controlling light increases further to $4.76 \times 10^5\,\mathrm{W/\mu m^2}$, $7.14 \times 10^5\,\mathrm{W/\mu m^2}$, and $9.52 \times 10^5\,\mathrm{W/\mu m^2}$, the first peak shifts to 967 nm, 1006 nm, and 1046 nm and the second peak shifts to 1133 nm, 1151 nm, and 1165 nm. In order to know how these peaks change with the power density of the controlling light, we plot the wavelength of the first peak as a function of power of the controlling light in Fig. 4.

From Fig. 4 we can see that the wavelength of the first peak (γ_{peak}) increases linearly with the power density of the controlling light, following $\gamma_{\mathrm{peak}} = 94.715I + 928.768$. Hence, we can tune the transmission spectrum of the signal light continuously by adjusting the power of the controlling light. Thus, a tuneable nano-device is realized.

Generally, the mechanism of the EOT phenomenon can be considered as the coupling of surface plasmon resonance (SPR) and local surface plasmon (LSP)[6]. The incident light generates the diffraction wave in the subwavelength structure that satisfies the phase condition, thus excites SPR and enhances transmission at a specific resonance wavelength[2–4]. At the same time, the resonance of the

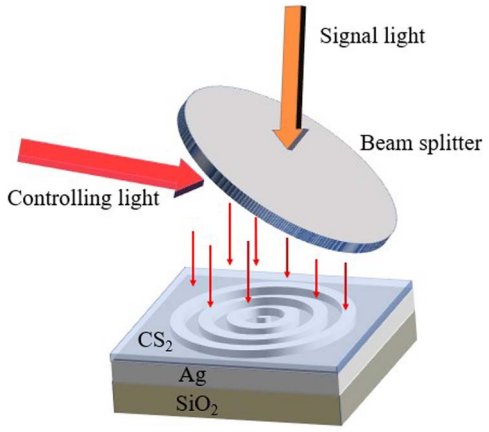

Fig. 2. Schematic diagram of the regulation strategy.

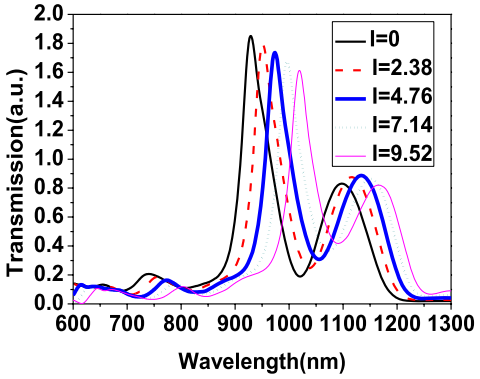

Fig. 3. Transmission spectra of the signal light under different powers of controlling light.

local waveguide affects the central wavelength and the peak of transmission spectrum. The redshift of the transmission spectrum can be explained by the interaction between incident light in a medium and surface plasmon on a metal surface. In this Letter, the dielectric constant of the nonlinear medium effectively increased with the power of the controlling light. In this condition, the incident signal photons with lower energy can satisfy the resonance condition and realize the coupling with surface plasmon. So the positions of the resonance peaks shifted to longer wavelengths.

In addition, multiple peaks in the transmission spectrum can be considered as the dominating effect of surface plasmon and local surface plasmon, respectively. The transmission spectra of both modes are nonlinearly related to the permeability of the medium[5]. Therefore, when the third-order magnetic permeability of carbon disulfide was changed by the controlling light, the transmission peaks dominated by the two resonance modes exhibited different transmittances. So, the height of peaks in the transmission spectrum varied irregularly with the power of the controlling light.

As discussed above, plane light can realize a tuneable device. However, in the view of application, the laser is the best choice. Usually, the transverse mode of the laser pulses was nearly Gaussian. Hence, we further simulated the transmission of the structure under the laser as the controlling light. In this case, the nonlinear

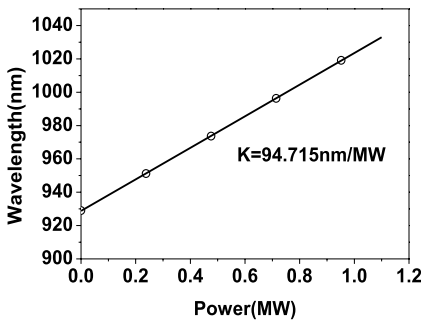

Fig. 4. Wavelength of the primary transmission peak under different powers of controlling light.

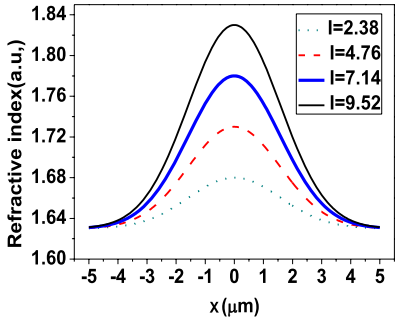

Fig. 5. X axis distribution of the refractive index.

refractive index of CS_2 will show a transverse Gaussian distribution

$$n = n_0 + \gamma I \exp[-\sigma(x^2 + y^2)], \tag{2}$$

where x and y are coordinate parameters, I is the center power of the Gaussian beam, and σ is a characteristic parameter of a Gaussian beam (herein, we chose $\sigma = 0.2$). The spatial distribution of the refractive index of CS_2 under the Gaussian beam is shown in Fig. 5.

By using FDTD, we simulated the transmission spectra under the Gaussian controlling light with the center power density of $0\,\mathrm{W/\mu m^2}$, $2.38\times10^5\,\mathrm{W/\mu m^2}$, $4.76\times10^5\,\mathrm{W/\mu m^2}$, $7.14\times10^5\,\mathrm{W/\mu m^2}$, and $9.52\times10^5\,\mathrm{W/\mu m^2}$ in Fig. 6.

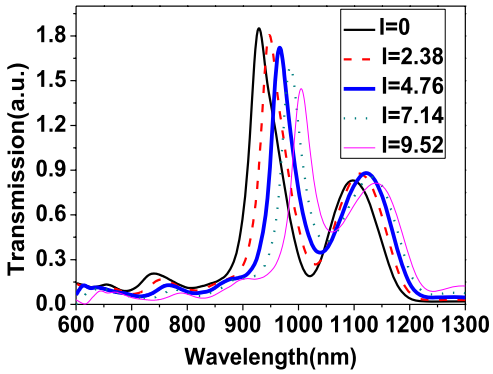

Fig. 6. Transmission spectra of the signal light under different powers of controlling light.

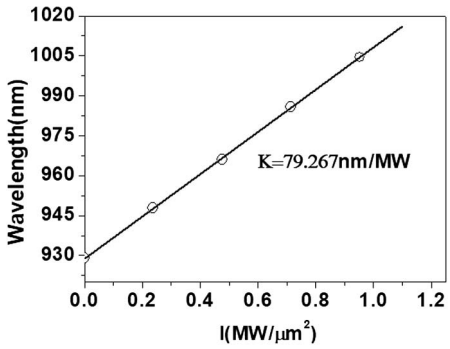

Fig. 7. Wavelengths of the primary transmission peak under different powers of controlling light.

In Fig. 6, with the increasing controlling light power, the first transmission peak wavelength redshifts from 930 nm to 949 nm, 966 nm, 984 nm, and 1008 nm, and the second peak from 1097 nm to 1109.53 nm, 1121.83 nm, 1130.94 nm, and 1139.04 nm. In addition, as shown in Fig. 7, the first peak also increases linearly with the increasing power density of the controlling light following $\gamma_{\mathrm{peak}} = 79.267I + 928.893$.

To summarize, a strategy to adjust the transmission of a subwavelength metal structure by employing external light was proposed. Specifically, we immersed the bullseye structure in a nonlinear medium and employed a controlling light to change the refractive index of the medium to adjust the wavelength of the transmission peak of the structure. By using FDTD, we verify the feasibility of our scheme. It is necessary for us to carry out experimental studies of the design in the future. In fact, we think the strategy can also be used in other structures. Furthermore, we infer that other forms of external fields such as electric fields, magnetic fields, and thermal fields may be used to adjust the transmission characteristics of subwavelength metal structures effectively via appropriate design. More research can be conducted.

This work was supported by the Natural Science Foundation of Heilongjiang Province (No. F2018027).

References

1. T. W. Ebbesen, H. J. Lezec, H. F. Ghaemi, T. Thio, and P. A. Wolff, Nature **391**, 667 (1998).
2. H. Ghaemi, T. Thio, D. Grupp, and T. Ebbesen, Phys. Rev. B **58**, 6779 (1998).
3. L. Martín-Moreno, F. J. García-Vidal, H. J. Lezec, K. M. Pellerin, T. Thio, J. B. Pendry, and T. W. Ebbesen, Phys. Rev. Lett. **86**, 1114 (2001).
4. E. Popov, M. Nevière, S. Enoch, and R. Reinisch, Phys. Rev. B **62**, 16100 (2000).
5. S. X. Xie, H. J. Li, H. Q. Xu, X. Zhou, S. L. Fu, and J. J. Wu, Sci. China Phys. Mech. Astron. **53**, 474 (2010).
6. K. J. K. Koerkamp, S. Enoch, F. B. Segerink, N. F. van Hulst, and L. Kuipers, Phys. Rev. Lett. **92**, 183901 (2004).
7. Z. Ruan and M. Qiu, Phys. Rev. Lett. **96**, 233901 (2006).
8. M. Najiminaini, F. Vasefi, B. Kaminska, and J. J. L. Carson, Plasmonics **8**, 217 (2013).
9. H. J. Lezec and T. Thio, Opt. Express **12**, 3629 (2004).
10. A. Degiron, H. J. Lezec, W. L. Barnes, and T. W. Ebbesen, Appl. Phys. Lett. **81**, 4327 (2002).
11. J. Wang, W. Zhou, and E.-P. Li, Opt. Express **17**, 20349 (2009).
12. K. Niu, Z. Huang, M. Li, and X. Wu, IEEE Trans. Antennas Propag. **65**, 7389 (2017).
13. A. P. Hibbins, J. R. Sambles, and C. R. Lawrence, Appl. Phys. Lett. **81**, 4661 (2002).
14. K. Niu, Z. Huang, M. Fang, M. Li, X. Li, and X. Wu, IEEE Access **6**, 14820 (2018).
15. K. Niu, Z. Huang, X. Ren, M. Li, B. Wu, and X. Wu, IEEE Trans. Antennas Propag. **66**, 6435 (2018).
16. U. Beaskoetxea, M. Beruete, M. Zehar, A. Agrawal, S. Liu, K. Blary, A. Chahadih, X.-L. Han, M. Navarro-Cia, D. Etayo, A. Nahata, T. Akalin, and M. S. Ayza, in *2014 8th International Congress on*

Advanced Electromagnetic Materials in Microwaves and Optics (2014), p. 55.
17. T. J. Heggie, D. A. Naylor, B. G. Gom, and E. V. Bordatchev, Proc. SPIE **8985**, 89851G (2014).
18. X. Lan, B. Cheng, Q. Yang, J. Huang, H. Wang, Y. Ma, H. Shi, and H. Xiao, Sens. Actuators B **193**, 95 (2014).
19. A. Karabchevsky, O. Krasnykov, I. Abdulhalim, B. Hadad, A. Goldner, M. Auslender, and S. Hava, Photon. Nanostruct. Fundam. Appl. **7**, 170 (2009).
20. M. H. Lee, H. Gao, and T. W. Odom, Nano Lett. **9**, 2584 (2009).
21. J. Zhang, M. Irannejad, M. Yavuz, and B. Cui, Nanoscale Res. Lett. **10**, 238 (2015).
22. L. Yu, X. Xiong, D. Liu, L. Feng, M. Li, L. Wang, G. Guo, G. Guo, and X. Ren, Chin. Opt. Lett. **15**, 082401 (2017).
23. J. Ma, D. Liu, J. Wang, and Z. Hu, Chin. Opt. Lett. **16**, 032301 (2018).
24. T. Thio, K. M. Pellerin, R. A. Linke, H. J. Lezec, and T. W. Ebbesen, Opt. Lett. **26**, 1972 (2001).
25. M. Sheik-Bahae, A. A. Said, T. H. Wei, D. J. Hagan, and E. W. Van Stryland, IEEE J. Quantum Electron. **26**, 760 (1990).
26. S. Couris, M. Renard, O. Faucher, B. Lavorel, R. Chaux, E. Koudoumas, and X. Michaut, Chem. Phys. Lett. **369**, 318 (2003).
27. H. J. Lezec, A. Degiron, E. Devaux, R. A. Linke, L. Martin-Moreno, F. J. Garcia-Vidal, and T. W. Ebbesen, Science **297**, 820 (2002).